eChem
https://www.sciltp.com/journals/eChem



Supplementary Materials

Disposable Screen-Printed Ca^{2+} Sensor Using NH_2-MIL-125@rGO as Solid-Contact Layer for Raw Milk Analysis

Wanting Zhang [1], Yunrui Fang [1], Qingbo An [1,*], Zhongqian Song [2], Bin Cai [3], Jing Sun [1,*] and Li Niu [4,*]

[1] Jilin Provincial International Joint Research Center of Photo-Functional Materials and Chemistry, School of Chemistry & Environmental Engineering, Changchun University of Science and Technology, Changchun 130022, China
[2] College of Medical Information and Artificial Intelligence, Shandong First Medical University & Shandong Academy of Medical Sciences, Jinan 250117, China
[3] School of Chemistry and Chemical Engineering, Shandong University, Jinan 250100, China
[4] School of Chemical Engineering and Technology, Sun Yat-sen University, Zhuhai 519082, China
* Correspondence: qban@cust.edu.cn (Q.A.); sjcust@126.com (J.S.); niuli@mail.sysu.edu.cn (L.N.)

How To Cite: Zhang, W.; Fang, Y.; An, Q.; et al. Disposable Screen-Printed Ca^{2+} Sensor Using NH_2-MIL-125@rGO as Solid-Contact Layer for Raw Milk Analysis. *eChem* **2026**, *2*(2), 12. https://doi.org/10.53941/echem.2026.100012

1. Materials and Methods

1.1. Apparatus

Scanning electron microscopy (SEM, sigma300, Zeiss, Cambridge, UK) and Transmission electron microscopy (TEM, Hitachi H-600, Hitachi, Tokyo, Japan) were appliedto observe the surface morphology and microstructure. X-ray photoelectron spectroscopy (XPS, Thermofisher ESCALAB Xi^+, Thermo Fisher Scientific, East Grinstead, UK) were performed to analyze chemical structures and surface elemental composition. X-ray diffraction (XRD, Bruker D8 Advance, Cu Kα source, λ = 1.54 Å, Bruker, Karlsruhe, Germany) was carried out to investigate the phase structure. The Raman spectra of GO, NH_2-MIL-125, and NH_2-MIL-125@rGO nanocomposites were obtained using a Renishaw RM2000 microscope (Renishaw, Gloucester, UK) operating at a laser excitation wavelength of 514.5 nm.

1.2. Preparation of Graphene Oxide

Add 100 mL concentrated sulfuric acid to a 250 mL round-bottomed flask containing 2 g graphite powder, stirring at room temperature for 3~4 h. Place it in an ice-water bath, add 6 g $KMnO_4$ uniformly, and the reaction becomes a paste after 12 h. Subsequently, add 100 mL of ultrapure water drop by drop and control the exothermic temperature at about 40 °C. Stir for another 3 h at room temperature, and finally pour the above solution into a large beaker and add 400 mL dilute hydrochloric acid, add H_2O_2 while stirring until the solution becomes light yellow, leave to precipitate, pour off the supernatant, wash the precipitate repeatedly with dilute hydrochloric acid, detect SO_4^{2-} in the supernatant with $BaCl_2$ solution to determine whether it contains Mn^{7+}, and finally centrifugal wash with acetone for three times, and then the product was transferred to the sample bottle, and added into the ultrapure water for backup.

2. Figures

The supplementary materials provide additional physicochemical characterization and electrochemical data for the NH_2-MIL-125@rGO composite and its application in Ca^{2+}-ISE. The supplementary data include elemental composition and distribution, X-ray photoelectron spectroscopy (XPS) analysis, electrochemical impedance spectroscopy (EIS), potentiometric performance, long-term stability, water-layer formation, measurement repeatability, morphological characterization, and surface wettability. Comparisons with previously reported Ca^{2+}-ISEs and the corresponding equivalent-circuit fitting parameters are also provided. Collectively, these results complement the findings presented in the main text and provide further support for the structural characterization and electrochemical evaluation of the developed electrode.

Copyright: © 2026 by the authors. This is an open access article under the terms and conditions of the Creative Commons Attribution (CC BY) license (https://creativecommons.org/licenses/by/4.0/).
Publisher's Note: Scilight stays neutral with regard to jurisdictional claims in published maps and institutional affiliations.

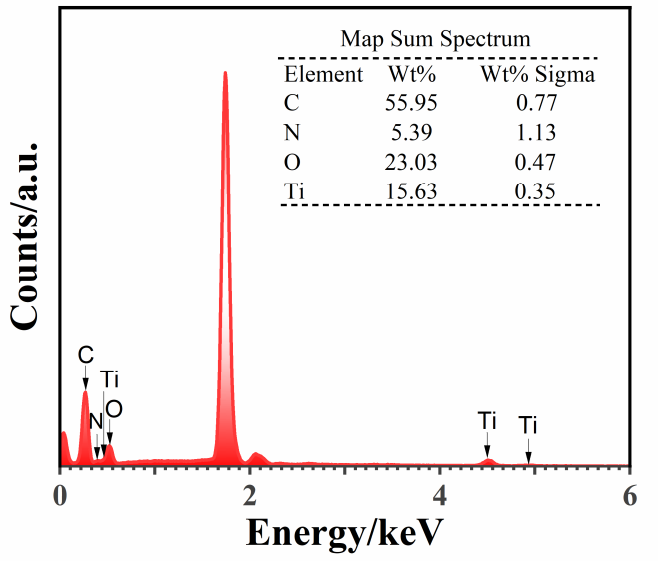


Figure S1. EDS and mass and atomic percentage elements of NH_2-MIL-125@rGO.

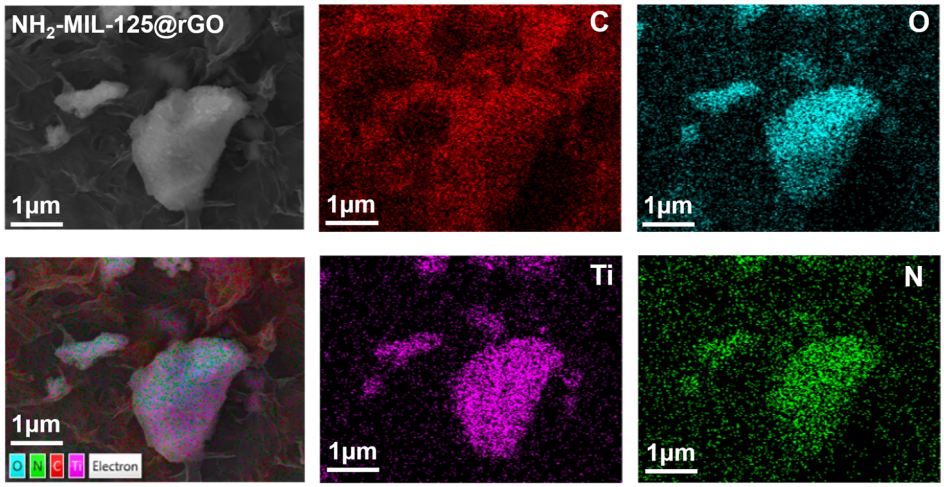


Figure S2. Elemental mapping images C, N, O and Ti in the NH_2-MIL-125@rGO.

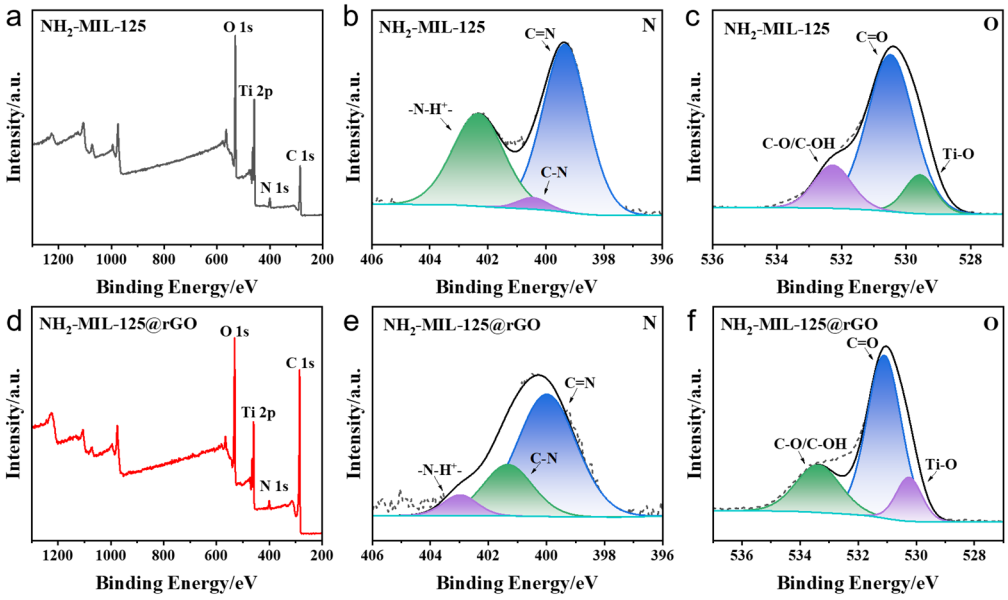


Figure S3. (**a**) XPS spectra of NH_2-MIL-125 and (**b**,**c**) XPS spectra of N 1s and O 1s at NH_2-MIL-125; (**d**) XPS spectra of NH_2-MIL-125@rGO and (**e**,**f**) XPS spectra of N 1s and O 1s for NH_2-MIL-125@rGO.

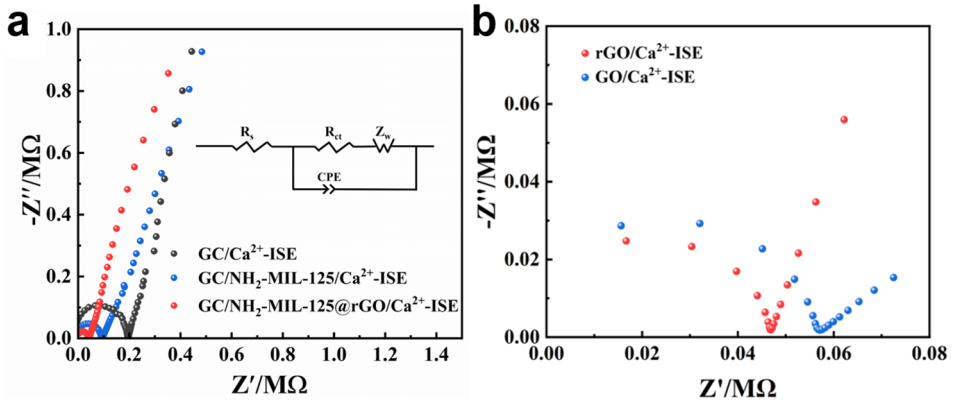


Figure S4. (**a**) Impedance spectra of Ca^{2+}-ISE, NH_2-MIL-125/Ca^{2+}-ISE and NH_2-MIL-125@rGO/Ca^{2+}-ISE in 0.1 M $CaCl_2$ aqueous solution. Insets represent the equivalent electrical circuits. R_s is the resistance of the solution. R_{ct} is the volume resistance of ISM and the contact resistance between the SC/ISM interface, controlling the semi-circle diameter. CPE is double-layer capacitance. Z_w is the "classical" finite-length Warburg impedance identified with the linear portion of the impedance spectra that appears at the lower frequencies [1]; (**b**) Impedance spectra of rGO/Ca^{2+}-ISE and GO/Ca^{2+}-ISE.

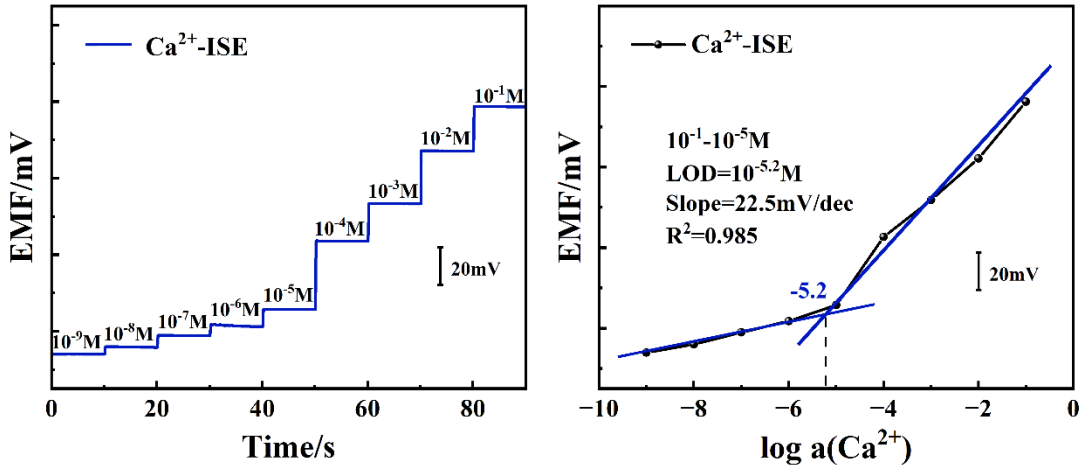


Figure S5. (**a**,**b**) Potential response and calibration curves of GC/Ca^{2+}-ISE to Ca^{2+} at concentrations ranging from 10^{-9}~10^{-1} M.

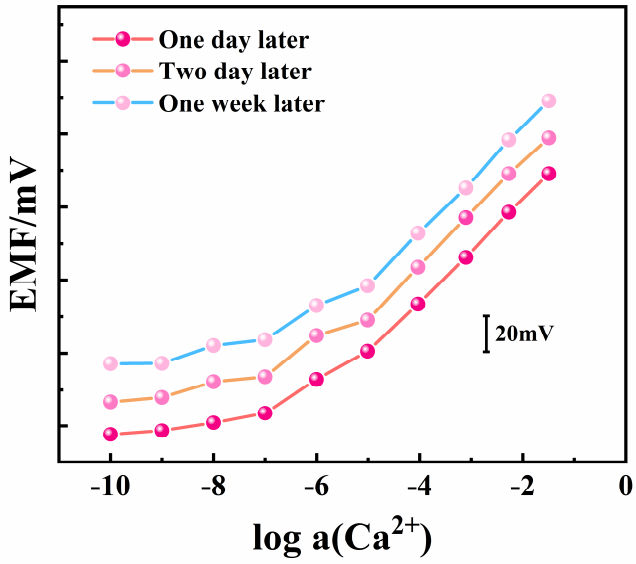


Figure S6. Potential response test of Ca^{2+} for seven consecutive days by NH_2-MIL-125@rGO/Ca^{2+}-ISE.

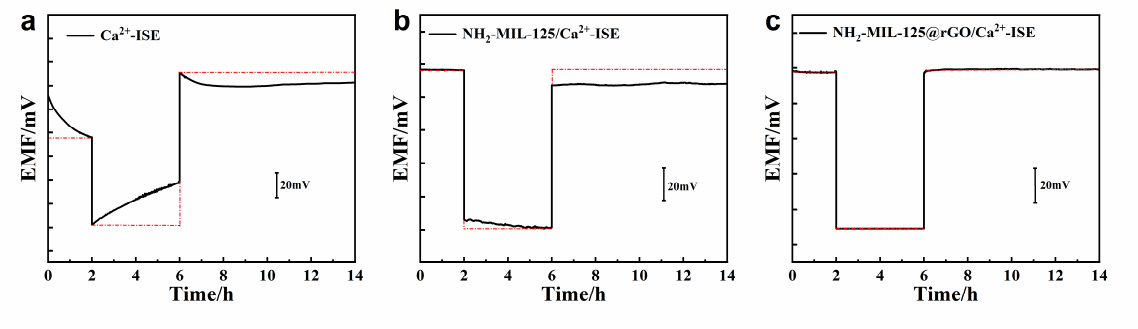


Figure S7. Aqueous test curves of (**a**) Ca^{2+}-ISE and (**b**) NH_2-MIL-125/Ca^{2+}-ISE and (**c**) NH_2-MIL-125@rGO/Ca^{2+}-ISE in 0.1 M $CaCl_2$ or 0.1 M NaCl solution (red lines are horizontal lines, The black line is the test line).

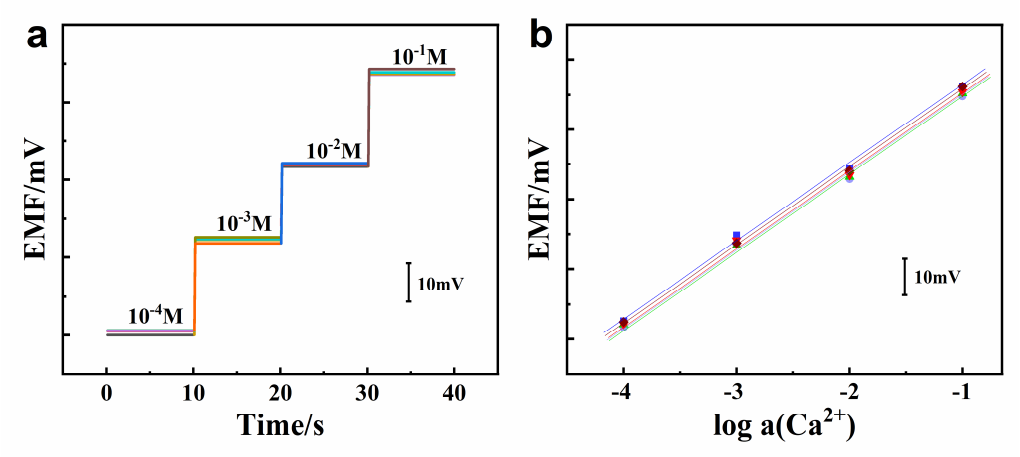


Figure S8. (**a**) NH_2-MIL-125@rGO/Ca^{2+}-ISE electrode potential response diagram repeated 5 times in 10^{-1}~10^{-4} M $CaCl_2$ solution and (**b**) potential calibration curve.

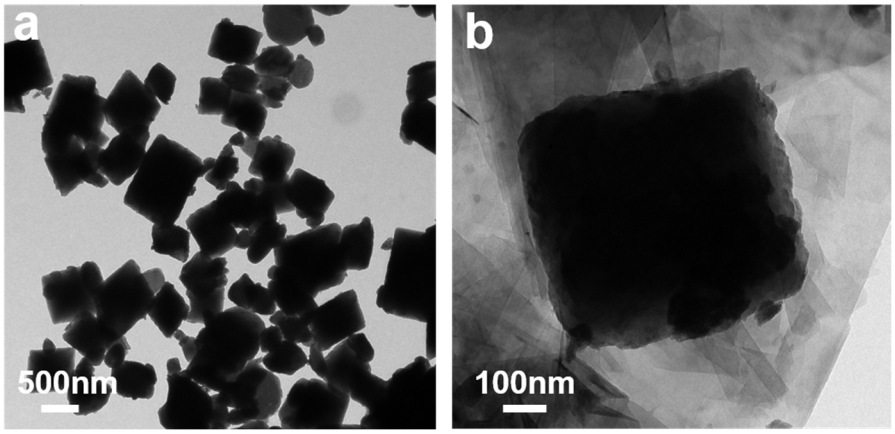


Figure S9. (**a**) TEM images of NH_2-MIL-125 and (**b**) NH_2-MIL-125@rGO.

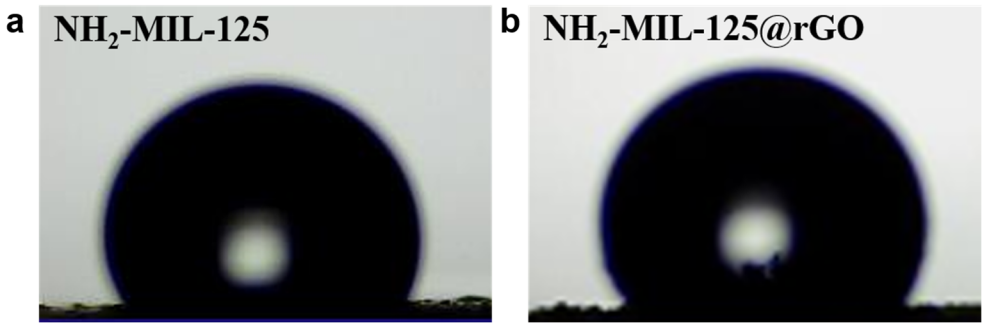


Figure S10. Water contact angle of (**a**)NH_2-MIL-125 and (**b**) NH_2-MIL-125@rGO.

Table S1. Comparison of the potentiometric performance of the NH_2-MIL-125@rGO based Ca^{2+}-ISEs with the reported other materials Ca^{2+}-ISEs.

Solid-Contact Materials	ISE	Potential Drift (μV/s)	Capacitance	Linear Range (M)	LOD (M)	Ref.
$NiCo_2S_4$	Ca^{2+}-ISE	1.7 μV/s	565 μF	10^{-6}–$10^{-1.5}$	$10^{-6.3}$	[2]
GO-ODA	Ca^{2+}-ISE	-	-	$10^{-6.5}$–10^{-3}	$10^{-6.8}$	[3]
MXene ($Ti_3C_2T_x$)	Ca^{2+}-ISE	4.0 μV/s	250 μF	$10^{-5.5}$–10^{-1}	$10^{-6.1}$	[4]
SWCNHs	Ca^{2+}-ISE	43.0 μV/s	23.26 μF	10^{-6}–10^{-2}	$10^{-6.1}$	[5]
rGO/Ag@AgCl/TMMCl	Ca^{2+}-ISE	5.87 μV/s	170.36 μF	10^{-6}–10^{-3}	$10^{-6.8}$	[6]
Ag@AgCl/TMMCl	Ca^{2+}-ISE	13.3 μV/s	75.2 μF	10^{-6}–10^{-2}	$10^{-6.5}$	[7]
NMC	Ca^{2+}-ISE	-	286.36 μF	10^{-6}–10^{-2}	$10^{-5.5}$	[8]
RGO	Ca^{2+}-ISE	-	38.61 μF	10^{-6}–10^{-2}	$10^{-5.6}$	[8]
CNT	Ca^{2+}-ISE	-	39.98 μF	10^{-6}–10^{-2}	$10^{-5.6}$	[8]
NH_2-MIL-125@rGO	Ca^{2+}-ISE	4.5 μV/s	222 μF	10^{-7}–10^{-1}	$10^{-7.2}$	This work

Notes: SWCNTs, single-walled carbon nanotubes; NMC, nitrogen-doped mesoporous carbon; RGO, reduced graphene oxide; CNT, Carbon nanotubes; GO-ODA, octadecylamine-functionalized graphene oxide; rGO/Ag@AgCl/TMMCl, reduced graphene oxide and Ag@AgCl/TMMCl composite; Ag@AgCl/TMMCl, core-shell Ag@AgCl nanoparticles and 1-tetradecyl-3-methylimidazolium chloride inorganic redox buffer; MXene, two-dimensional layered transition metal carbides/nitrides; $SHTi_3C_2$, superhydrophobic Ti_3C_2.

Table S2. Detection limits comparison of Ca^{2+}-ISE based on NH_2-MIL-125@rGO with solid contact ion-selective electrodes constructed with other MOF's composites.

Solid-Contact Materials	ISE	Linear Range (M)	LOD (M)	Ref.
BGO/AlFu MOF	Br^--ISE	10^{-7}–10^{-1}	$10^{-7.15}$	[9]
MWCNT/NPC	Ca^{2+}-ISE	10^{-8}–10^{-3}	$10^{-8.8}$	[10]
NH_2-MIL-125@rGO	Ca^{2+}-ISE	10^{-7}–10^{-1}	$10^{-7.2}$	This work

Table S3. The best equivalent circuit and the corresponding parameters for the developed electrodes were as follows.

Electrode	R_s	R_{ct}	CPE	Z_w
Ca^{2+}-ISE	−15,400	208,730	1.773×10^{-11}	6,482,900
NH_2-MIL-125/Ca^{2+}-ISE	−8371	100,030	6.606×10^{-11}	900,670
NH_2-125@rGO/Ca^{2+}-ISE	−4419	46,266	2.097×10^{-10}	1,309,500

References

1. Sundfors, F.; Bobacka, J. EIS Study of the Redox Reaction of $Fe(CN)_6^{3-/4-}$ at Poly(3,4-Ethylenedioxythiophene) Electrodes: Influence of DC Potential and cOx:cRed Ratio. *J. Electroanal. Chem.* **2004**, *572*, 309–316. https://doi.org/10.1016/j.jelechem.2003.12.013.
2. Li, Y.; Li, J.; Qin, W. All-Solid-State Polymeric Membrane Ion-Selective Electrodes Based on $NiCo_2S_4$ as a Solid Contact. *Anal. Chem.* **2022**, *94*, 3574–3580. https://doi.org/10.1021/acs.analchem.1c04748.
3. Yin, T.; Li, J.; Qin, W. An All-Solid-State Polymeric Membrane Ca^{2+}-Selective Electrode Based on Hydrophobic Alkyl-Chain-Functionalized Graphene Oxide. *Electroanalysis* **2017**, *29*, 821–827. https://doi.org/10.1002/elan.201600383.
4. Shao, Y.; Yao, Y.; Jiang, C.; et al. Two-Dimensional MXene Nanosheets (Types $Ti_3C_2T_x$ and Ti_2CT_x) as New Ion-to-Electron Transducers in Solid-Contact Calcium Ion-Selective Electrodes. *Microchim. Acta* **2019**, *186*, 750. https://doi.org/10.1007/s00604-019-3878-7.
5. Jiang, C.; Yao, Y.; Cai, Y.; et al. All-Solid-State Potentiometric Sensor Using Single-Walled Carbon Nanohorns as Transducer. *Sens. Actuators B Chem.* **2019**, *283*, 284–289. https://doi.org/10.1016/j.snb.2018.12.040.
6. Chai, D.; Sun, Y.; Li, Z.; et al. A Novel Inorganic Redox Buffer of R-GO/Ag@AgCl/TMMCl Utilized as an Effective Ion-to-Electron Transducer for a Solid Contact Calcium Ion-Selective Electrode. *Sens. Actuators B Chem.* **2022**, *367*, 132055. https://doi.org/10.1016/j.snb.2022.132055.
7. Zeng, X.; Qin, W. A Solid-Contact Ca^{2+}-Selective Electrode Based on an Inorganic Redox Buffer of Ag@AgCl/1-Tetradecyl-3-Methylimidazolium Chloride as Ion-to-Electron Transducer. *Talanta* **2020**, *209*, 120570. https://doi.org/10.1016/j.talanta.2019.120570.
8. Zhang, Y.; Tang, Y.; Liang, R.; et al. Carbon-Based Transducers for Solid-Contact Calcium Ion-Selective Electrodes: Mesopore and Nitrogen-Doping Effects. *Membranes* **2022**, *12*, 903. https://doi.org/10.3390/membranes12090903.
9. Kaur, N.; Kaur, J.; Badru, R.; et al. BGO/AlFu MOF Core Shell Nano-Composite Based Bromide Ion-Selective Electrode. *J. Environ. Chem. Eng.* **2020**, *8*, 104375. https://doi.org/10.1016/j.jece.2020.104375.
10. Xu, J.; Sun, Z.; Li, F.; et al. Nitrogen-Doped Porous Carbon Derived from Zeolitic Imidazolate Framework-67 Strung into Necklace with Carbon Nanotubes for the Detection of Calcium at Ultralow Level. *J. Electrochem. Soc.* **2020**, *167*, 087512. https://doi.org/10.1149/1945-7111/ab91cb.